Nicotinamide riboside, a form of vitamin B₃, protects against excitotoxicity-induced axonal degeneration

Pauline Vaur,* Bernard Brugg,* Mathias Mericskay,*,[†] Zhenlin Li,*,[‡] Mark S. Schmidt,[§] Denis Vivien,[¶] Cyrille Orset,[¶] Etienne Jacotot,* Charles Brenner,[§] and Eric Duplus*,[1]

*Unité Mixte de Recherche (UMR) Adaptation Biologique et Vieillissement (UMR 8256), Institut Biologie Paris Seine, Centre National de la Recherche Scientifique (CNRS), INSERM, Université Pierre et Marie Curie (UPMC), Sorbonne Universités, Paris, France; [‡]Equipe de Recherche Labellisée (ERL) U1164 and [†]Unité Signalisation et Physiopathologie Cardiovasculaire, INSERM, Université Paris–Saclay, Université Paris Sud, Châtenay-Malabry, France; [§]Department of Biochemistry, Carver College of Medicine, University of Iowa, Iowa City, Iowa, USA; and [¶]Unité INSERM 1237, GIP Cycéron, Centre Hospitalier Universitaire de Caen, Université Caen Normandie, Caen, France

ABSTRACT: NAD$^+$ depletion is a common phenomenon in neurodegenerative pathologies. Excitotoxicity occurs in multiple neurologic disorders and NAD$^+$ was shown to prevent neuronal degeneration in this process through mechanisms that remained to be determined. The activity of nicotinamide riboside (NR) in neuroprotective models and the recent description of extracellular conversion of NAD$^+$ to NR prompted us to probe the effects of NAD$^+$ and NR in protection against excitotoxicity. Here, we show that intracortical administration of NR but not NAD$^+$ reduces brain damage induced by NMDA injection. Using cortical neurons, we found that provision of extracellular NR delays NMDA-induced axonal degeneration (AxD) much more strongly than extracellular NAD$^+$. Moreover, the stronger effect of NR compared to NAD$^+$ depends of axonal stress since in AxD induced by pharmacological inhibition of nicotinamide salvage, both NAD$^+$ and NR prevent neuronal death and AxD in a manner that depends on internalization of NR. Taken together, our findings demonstrate that NR is a better neuroprotective agent than NAD$^+$ in excitotoxicity-induced AxD and that axonal protection involves defending intracellular NAD$^+$ homeostasis.—Vaur, P., Brugg, B., Mericskay, M., Li, Z., Schmidt, M. S., Vivien, D., Orset, C., Jacotot, E., Brenner, C., Duplus, E. Nicotinamide riboside, a form of vitamin B₃, protects against excitotoxicity-induced axonal degeneration. FASEB J. 31, 5440–5452 (2017). www.fasebj.org

KEY WORDS: NAD$^+$ · NMDA · FK866 · cortical neurons · NR

Axonal degeneration (AxD) is an early major event in acute cerebral injury and in chronic neurodegenerative diseases, including Alzheimer and Parkinson diseases (1–4). Preserving axonal integrity by stopping neurodegenerative expansion and preventing irreversible neuronal damage could represent a powerful therapeutic strategy in prevention of brain disorders. Several lines of reasoning support AxD proceeding *via* a mechanism associated with dysregulated NAD$^+$ metabolism that is distinct from neuronal cell body death (5–8). Notably, a spontaneous mutation termed *Wlds*, which delays axotomy-induced AxD in neurons derived from the peripheral nervous system (PNS), has been discovered in mice (9). *Wlds* encodes a fusion protein that overexpresses and stabilizes the complete coding sequence of nicotinamide mononucleotide adenylyltransferase (Nmnat)-1, an enzyme that converts nicotinamide mononucleotide (NMN) to NAD$^+$ (10). Moreover, several studies revealed a protective effect of Nmnat overexpression or application of NAD$^+$ or NAD$^+$ precursors in axotomy-induced AxD in the PNS (5, 7, 8, 11). One such precursor, nicotinamide riboside (NR), protects against diabetic peripheral neuropathy *in vivo* (12).

The molecular cascade and the time course of events in AxD have been explored intensively. Axonal lesion in dorsal root ganglia induces a loss of Nmnat2 protein and activation of sterile α and TIR motif–containing (Sarm)-1 protein, thereby triggering the MAPK signaling pathway, NAD$^+$ depletion and subsequent AxD (13–15). More recently, it has been shown that Nmnat1 expression can

inhibit Sarm1-mediated NAD$^+$ depletion (16). These results highlight the essential role of NAD$^+$ metabolism in AxD of PNS-derived neurons. Whether a similar relationship exists between NAD$^+$ metabolism and AxD in the CNS has not been well explored.

A strong NAD$^+$ depletion in neurons has been revealed during excitotoxicity (17–20). Excitotoxicity is a common process taking place in most neurodegenerative disorders affecting the CNS and is the main cell death mechanism in ischemia and hypoxia. Moreover, excitotoxicity has been shown to induce AxD in CNS-derived neurons (21, 22). The involvement of NAD$^+$ in excitotoxic stress was confirmed by studies demonstrating a neuroprotective effect of NAD$^+$ repletion *via* overexpression of NAD$^+$ biosynthetic enzymes, application of extracellular NAD$^+$ or its precursors (17, 19, 23).

In the CNS, it has not been determined whether NAD$^+$ functions as a neurotransmitter or as a source of intracellular NAD$^+$ in protecting against excitotoxicity-induced AxD. This mechanistic understanding is needed in pursuing therapeutic strategies with either NR or NAD$^+$. Because NAD$^+$ contains 2 phosphate groups, transport across the plasma membrane is not expected, such that the protective effect of extracellular NAD$^+$ may be related to extracellular conversion to NR, one of its biosynthetic precursors (24–28). This extracellular conversion pathway is mediated by ecto-nucleotide pyrophosphatase/phosphodiesterase (ENPPase) and ectonucleotidase (ENTase) activities, previously characterized for extracellular ATP conversion (29). After NAD$^+$ and NMN are converted to NR extracellularly, NR is used intracellularly through the NR kinase pathway (28, 30).

NR is a recently described vitamin precursor of NAD$^+$ that is found in milk (31, 32) and is orally available in humans (33). It enters cells through nucleoside transporters (NTs) and is converted to NMN and NAD$^+$ through the successive action of NR kinases (Nmrk1/2) and Nmnat isozymes (28). *In vitro*, NR delays AxD after axotomy in dorsal root ganglion neurons (7). In mice, NR prevents cognitive decline and amyloid-β peptide aggregation (34), protects against noise-induced neurite retraction of inner hair cells and hearing loss (35), and protects against diabetic peripheral neuropathy (12). In rats, NR both protects and reverses chemotherapeutic peripheral neuropathy (36). We performed a comparative study of NAD$^+$ and NR and examined NAD$^+$ extracellular conversion in cortical neurons during excitotoxic stress. We found that NR has a strong protective effect on NMDA-induced neurodegeneration both *in vitro* and *in vivo*. More specifically, NR, but not NAD$^+$, had a strong effect on NMDA-induced AxD, involving a local NR metabolism within the axon. Finally, we showed that NAD$^+$ efficiency in cortical AxD protection is limited by conversion to NR.

MATERIALS AND METHODS

Microfluidic chip production

The 3-compartment chip master was constructed as described in Kanaan *et al.* (37). For chip production, polydimethylsiloxane

(Sylgard 184, PDMS; Dow Corning, Midland, MI, USA) was mixed with a curing agent (9:1 ratio) and degassed under a vacuum. The resulting preparation was poured onto a polyester resin replicate and reticulated at 70°C for at least 2 h. The elastomeric polymer print was detached, and 2 reservoirs were punched for each macrochannel. The polymer print and a glass coverslip, cleaned with isopropanol and dried, were treated for 3 min in an air plasma generator (98% power, 0.6 mbar; Diener Electronic, Ebhausen, Germany) and bonded together. The chips were placed under UV for 20 min and then coated with a solution of poly D-lysine (10 µg/ml, P7280; Millipore-Sigma, St. Louis, MO, USA) overnight and washed with Dulbecco-PBS (D-PBS) (14190169; Thermo Fisher Scientific, Waltham, MA, USA) before cell seeding. Alternatively, 3-compartment chips were purchased from Microbrain Biotech (Paris, France).

Primary neuronal culture

All animals were ethically maintained and used in compliance with the European Policy on Ethics. Cortices were microdissected from E14 embryos of Swiss mice (Janvier, Le Genest Saint Isle, France) in D-PBS supplemented with 0.1% (w/v) glucose (Thermo Fisher Scientific). C57BL/6N mice were used in *Nmrk2*-knockout (KO) experiments. Dissected structures were digested with papain (15 U/ml in DMEM; 76220; Millipore-Sigma) for 5 min at 37°C. After papain inactivation with 10% (v/v) fetal bovine serum (GE Healthcare, Little Chalfont, United Kingdom), structures were mechanically dissociated with a pipette in DMEM Glutamax-1 (31966; Thermo Fisher Scientific) containing DNAse-I (D5025, Millipore-Sigma). After 2 7 min centrifugations at 700 *g*, cells were resuspended in a medium containing DMEM Glutamax-1, penicillin (100 U/ml)/streptomycin (100 µg/ml) (15140; Thermo Fisher Scientific), 5% (v/v) fetal bovine serum, N2 supplement (17502048; Thermo Fisher Scientific), and B-27 supplement (17504-044; Thermo Fisher Scientific) to a final density of 50 million cells/ml. Cortical cells were then seeded in the somatic compartment. Cell culture medium was added equally to the 4 reservoirs. Microfluidic chips were placed in Petri dishes containing 10% EDTA (Millipore-Sigma) and incubated at 37°C in a 5% CO_2 atmosphere. The culture medium was renewed every 6 d. Upon differentiation, cortical axons entered the microchannels and reached the second chambers after 4–5 d. Cortical axons continued growing thereafter.

Nmrk2-KO mouse

Nmrk2-KO mice were obtained by the injection of embryonic stem cells (Nmrk2$^{tm1(KOMP)Vlcg}$ allele) from the Knockout Mouse Project (KOMP) into C57BL/6N blastocysts at Centre National de la Recherche Scientifique–Transgenesis, Archiving and Animal Models (CNRS–TAAM) Transgenic Animal Facility (SEAT; Villejuif, France). All exons and introns of the *Nmrk2* gene are replaced by a *lacZ* reporter gene to create a null allele in embryonic stem cells (University of California, Davis, Davis, CA, USA; *https://www.komp.org/geneinfo.php?geneid=65082*). Chimeric male mice were used to obtain heterozygous *Nmrk2*-mutant mice on a C57BL/6N background. Homozygous *Nmrk2*-KO mice were viable and fertile. We validated the deletion by sequencing the genomic DNA from the KO mice.

Pharmacological treatments

Cells were pretreated and/or treated between 11 and 13 d *in vitro*. To ensure fluidic isolation, a differential hydrostatic pressure between compartments was maintained.

The following compounds were used: NMDA, (100 µM; M3262; Millipore-Sigma), FK866 (10 µM; F8557; Millipore-Sigma), NAD$^+$ (N3014; Millipore-Sigma), NMN (N3501;

Millipore-Sigma), NR (ChromaDex, Irvine, CA, USA), NAM (N0636; Millipore-Sigma), dipyridamole (DP, 50 µM; D9766; Millipore-Sigma), cytidine monophosphate (CMP; 25 mM; C1006; Millipore-Sigma), and (+)MK-801-maleate (10/50 µM; 0924; Tocris Bioscience, Bristol, United Kingdom).

Immunofluorescence detection and image acquisition

At various times, cultures were fixed with 4% (w/v) para-formaldehyde (15714-S; Euromedex, Souffelweyersheim, France) +4% (w/v) sucrose (S0389; Millipore-Sigma) for 20 min at room temperature. Cells were then washed once with PBS for 10 min and permeabilized for 30 min with D-PBS containing 0.2% (v/v) TritonX-100 (Millipore-Sigma) and 1% (w/v) BSA (Millipore-Sigma). Immunostaining was performed as described in Magnifico *et al.* (6) using the following conjugated antibodies diluted in D-PBS: anti-βIII tubulin-Alexa Fluor 488 (1:500, AB15708A4; Millipore-Sigma) and anti-microtubule-associated protein 2 (MAP2)-Alexa 555 (1:500, MAB3418A5; Millipore-Sigma). Cell nuclei were stained by using Hoechst 33342 (2 µg/ml). The chips were then rinsed once with PBS and filled with PBS+0.1% sodium azide.

Images were acquired with an Axio-observer Z1 microscope (Zeiss, Wetzlar, Germany) fitted with a cooled CCD camera (CoolsnapHQ2; Roper Scientific, Trenton, NJ, USA). The microscope was controlled with Metamorph (Berlin, Germany) software, and images were analyzed with ImageJ software (National Institutes of Health, Bethesda, MD, USA).

Quantification of axonal fragmentation and neuronal death

Axonal fragmentation was assessed with a macro developed in ImageJ software that contained the following steps: *1*) subtract background, *2*) plug in tubeness (σ = 1), *3*) plug in Otsu thresholding, and *4*) analyze particles by measuring total particle area (A_{TOTAL}) and identifying particles with circularity higher than 0.2 ($A_{0.2}$). The fragmentation index is obtained as the ratio $A_{0.2}/A_{TOTAL}$. This index is almost linearly correlated with fragmented axon percentages: indices under 0.2, ~0.5, and up to 0.8 correspond to <10, 50, and more than 90% of fragmented axons, respectively. Neuronal death was quantified by calculating the ratio of condensing nuclei to total nuclei.

PCR and real-time quantitative PCR

Primary cortical neurons were lysed at DIV 11, and tissues were lysed from 8-wk-old mice. Three wells were pooled to obtain 1 sample. Total RNA was isolated with an RNeasy kit (74104; Qiagen, Valencia, CA, USA) according to the manufacturer's protocol. From the total RNA, 1 µg was RNase free-DNase treated and retrotranscribed with a SuperScript II reverse transcriptase kit (18064-022; Thermo Fisher Scientific) according to the manufacturer's instruction. The remaining RNA was hydrolyzed using RNase H from *E. coli* (AM2293; Thermo Fisher Scientific).

PCR amplification was performed in a thermocycler by mixing 2 µl of cDNA with 0.5 µM of forward and reverse nucleotide sequences (**Table 1**) in a PCR buffer containing dNTP mix (200 µM each), MgCl$_2$ (1.5 mM), and 0.5 U of Taq DNA polymerase (18038; Thermo Fisher Scientific). Initially, the template was denatured by heating to 95°C for 5 min, followed by 30 amplification cycles. Each cycle consisted of 3 steps: the first for 45 s at 94°C, the second for 30 s at annealing temperature (depending of the amplified mRNA), and the third for 1 min at 72°C for polymerization. The final step was an extension at 72°C for 10 min. PCR products were electrophoresed on 1.5% (w/v) agarose gel and stained with ethidium bromide (0.5 µg/ml).

Quantitative PCR was performed with a LightCycler480 (Roche Applied Science, Penzberg, Germany), by mixing 1:50 diluted cDNA with the target-specific primers and Light Cycler 480 SYBRGreen I Master mix (4707516001; Roche, Basel, Switzerland) according to the manufacturer's instructions. Amplification conditions were initial denaturation for 5 min at 95°C followed by 40 cycles of 10 s at 95°C, 15 s at annealing temperature and 10 s at 72°C. Results were analyzed with LightCycler 480 SW 1.5 software. Individual PCR products were analyzed by melting-point analysis. The expression level of a gene was normalized relative to that of mouse β-actin or hypoxanthine-guanine phosphoribosyltransferase (*HPRT*).

NAD$^+$ assay

NAD$^+$ was measured using EnzyChrom NAD$^+$/NADH Assay Kit (E2ND-100; Euromedex) according to the manufacturer's protocol. Targeted quantitative NAD$^+$ metabolomics were performed as described in Trammell and Brenner (38).

In vivo NMDA-induced excitotoxicity experiments

Experiments were performed on male C57/BL6 mice (23 ± 3 g, produced and provided by GIP Cycéron animal facilities) in accordance with European Union Directives (210/63/UE) and French Ethics laws (R214; 87-137; Ministère de l'Agriculture) on animal experimentation and were approved by the Université Caen Normandie Animal Welfare Committee. Mice were deeply anesthetized with isoflurane 5% and maintained under

TABLE 1. *PCR primer sequences*

Gene	Forward	Reverse	Size (pb)	T_a
	Primer, 5'- 3'		
β-Actin	AGCCATGTACGTAGCCATCC	CTCTCAGCTGTGGTGGTGAA	228	63
HRPT	ATTATGCCGAGGATTTGGAA	CCCATCTCCTTCATGACATCT	94	60
ENT1	AGCCTGTGCAGTTGTCATTTT	TCTTCCTTTTGGCTCCTCTCC	153	60
ENT2	CGAGTCGGTGCGGATTCTG	GCACGGCACAGAAGGAATTG	149	60
ENT3	ATAGCAGCGTTTACGGCCTC	CACTGGATGCTGCCAGGTC	127	60
ENT4	TTTGGCAGTGTGCCCATGA	TGCAGTAGGCCACAGCAGAG	127	60
Nmrk1	AGGGAAGACGACACTGGCTA	AGCGCTTCAAGCACATCATA	141	63
Nmrk2	CACCTCAGGACCAGTCACCT	CTGTTGGTCAGGGTGGTCTT	94	60
Nmnat1	TTCAAGGCCTGACAACATCGC	GAGCACCTTCACAGTCTCCACC	94	60
Nmnat2	CAGTGCGAGAGACCTCATCCC	ACACATGATGAGACGGTGCCG	94	60
Nmnat3	GGTGTGGAGGTGTGTGACAGC	GCCATGGCCACTCGGTGATGG	94	60

anesthesia with 2% isoflurane in a 70/30% gas mixture (N_2O/O_2) during surgery. The rectal temperature was maintained at 37 ± 0.5°C throughout the surgical procedure using a feedback-regulated heating system.

A cortical unilateral injection [coordinates: 0.5 mm posterior, 2.0 mm lateral, −0.5 mm ventral to the bregma (39)] of NMDA (5 nmol; in 0.33 µl), coinjected or not with NAD^+ or NR (50 nmol) was performed after placing the animals in a stereotaxic frame. Solutions were injected by the use of a micropipette made with hematologic micropipettes (calibrated at 15 mm/µl, assistant ref 555/5; Hecht, Sondheim-Rhoen, Germany). The micropipette was removed 3 min later. The volume of the lesion was analyzed 48 h later.

MRI

Experiments were performed on a Pharmascan 7T (Bruker, Bremen, Germany). T2-weighted images were acquired with a multislice multiecho sequence: TE/TR 51.3/2500 ms 48 h after injection. Lesion volumes were quantified on MRI with ImageJ software.

Statistical analysis

Differences were assessed by a Mann-Whitney U test to compare 2 conditions or a Kruskal-Wallis test to compare >2 conditions.

RESULTS

NMDA treatment on neuronal cell bodies induces neuronal death and axonal degeneration

To dissect the protective effects of NAD^+ and NR on AxD, we cultured cortical neurons in microfluidic devices containing 3 chambers connected to each other (37). When seeded in the left chamber, cortical neurons projected their axons from the proximal to the distal chamber through asymmetric filtering microchannels, whereas the somata and dendrites were confined in the left chamber. As a consequence of such compartmentalization, the right chamber of the microfluidic device contained only axons. When depressurized, the central chamber acts as siphon and ensures optimal fluidic isolation of the distal axonal and somatodendritic chambers (**Fig. 1A, B**).

Analysis of dendrites (MAP2, red), nuclear chromatin (Hoechst 33342, blue), and axons (β3-tubulin) indicated that the seeded cortical neurons were healthy after 2 wk in culture (Fig. 1C). Somatodendritic application of 100 µM NMDA in the proximal chamber induced dendrite degeneration marked by a loss of MAP2 immunostaining and nuclear condensation associated with a severe AxD visualized by punctiform β3-tubulin immunostaining in the distal chamber (Fig. 1C–G). By contrast, local application of NMDA to axons in the distal chamber had no effect on neurons, consistent with the fact that NMDA receptors (NMDARs) are exclusively localized to the somatodendritic compartment (22) (Fig. 1E–G). NMDAR involvement in NMDA-induced neurodegeneration was confirmed with the noncompetitive NMDAR antagonist

MK-801. Nuclear condensation and AxD after 8 h NMDA treatment were fully blocked by coaddition of 10 or 50 µM MK-801 (Fig. 1H, I).

NR has a stronger neuroprotective effect than NAD+ during excitotoxicity, both *in vitro* and *in vivo*

To evaluate and compare the potential neuroprotective properties of NAD^+ and NR, cortical neurons were treated with 100 µM NMDA in the presence or absence of 5 mM NAD^+ or 1 mM NR. Nuclear condensation and AxD were then quantified over time. As shown in **Fig. 2A**, after 24 h of treatment, no inhibition of dendrite degeneration (MAP2) nor inhibition of nuclear condensation was observed after NAD^+ or NR treatment, whereas both molecules delayed AxD (Fig. 2A–C). NAD^+ protection was weak (67% of protection compared to NMDA effect after 8 h of treatment, 22% after 24 h), whereas NR fully protected axons after 8 h and still provided 72% protection 24 h after NMDA treatment (Fig. 2C). NAD^+ and NR efficiencies were also compared in a dose–range assay in cortical neurons cotreated with 100 µM NMDA for 24 h (Fig. 2D). NAD^+ started to delay AxD from 5 mM. In contrast, NR was efficient at a 10-fold lower dose (0.5 mM; 33 *vs.* 43% of protection) with a maximum protective activity at 1 mM. We asked whether the absence of protection of NAD^+ and NR on NMDA-induced nuclear condensation was due to the high-dose of NMDA (100 µM) leading to irretrievable degeneration. Accordingly, we challenged 5 mM NAD^+ or 1 mM NR with a lower 10 µM NMDA concentration during 24 h (Supplemental Fig. S1). A lower nuclear condensation was observed with 10 µM NMDA (30%) compared with that obtained with 100 µM NMDA (53%) but neither NAD^+ nor NR had any protective effect on this phenomenon.

Considering the different neuroprotective activities of NAD^+ and NR in our *in vitro* model of excitotoxicity, we asked if NAD^+ and NR could be neuroprotective in an *in vivo* setting of excitotoxicity. For this purpose, we coinjected NMDA (5 nmol) and NAD^+ or NR (50 nmol each) into mouse cortical structures as published (40). Strikingly, the volume of the NMDA-induced lesion as measured by MRI was significantly reduced after NR coinjection, whereas NAD^+ did not reveal a significant protection (Fig. 2E, F). Thus, NR has a more potent neuroprotective effect than NAD^+ in NMDA-induced neurodegeneration, both *in vitro* and *in vivo*.

NR is a more powerful brain NAD+-boosting compound than NAD+

We performed targeted quantitative NAD^+ metabolomics to evaluate the effect of NR and NAD^+ on NMDA-treated mouse brains (38). As shown in Fig. 2G, NR significantly elevated brain NAD^+ from <400 pmol/mg to nearly 500 pmol/mg, whereas the increase in brain NAD^+ from NAD^+ injection was not significant. Consistent
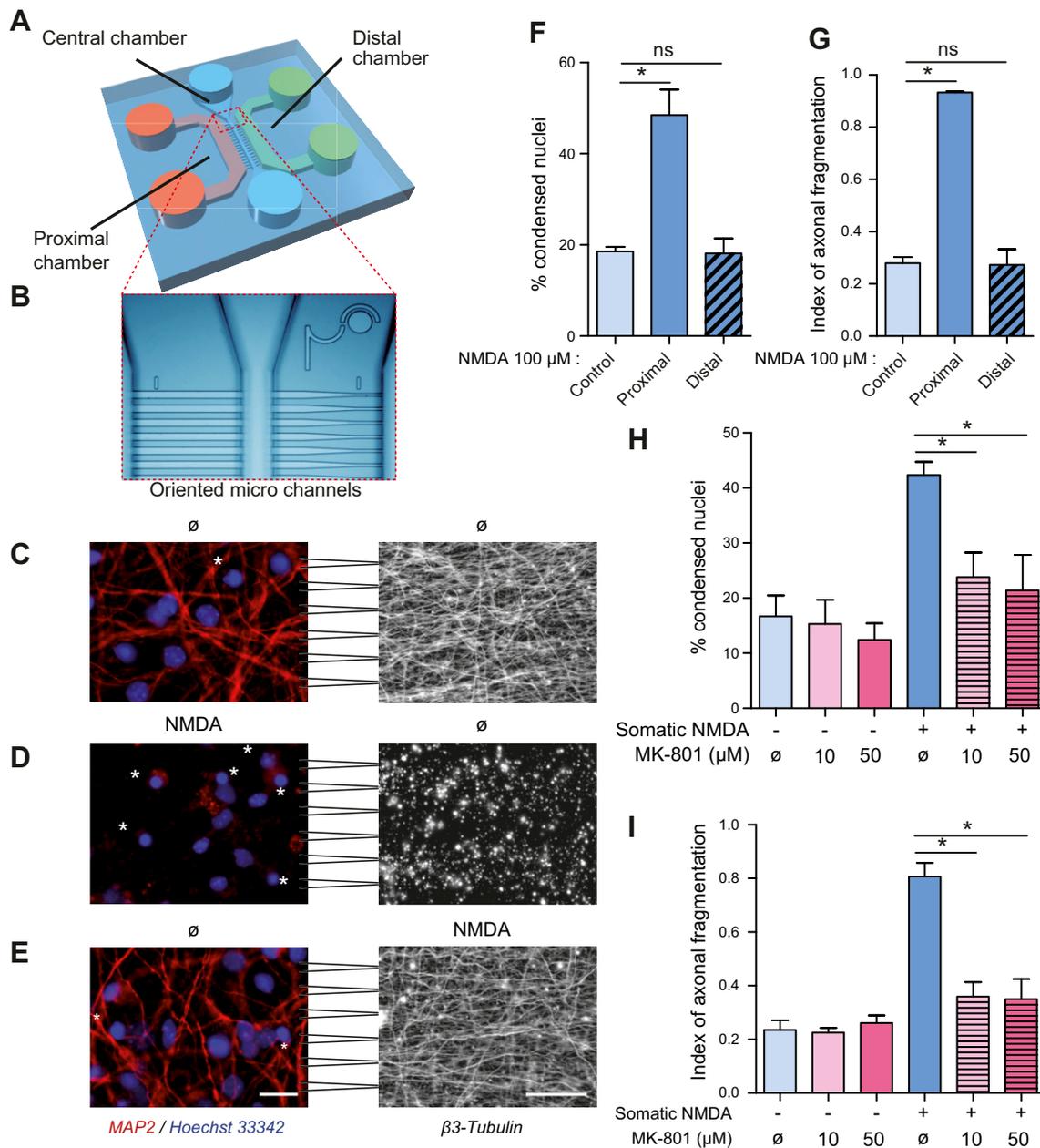
Figure 1. Somatic application of NMDA on cortical neurons induces neuronal death and axonal degeneration. *A)* 3-dimensional representation of microfluidic devices composed of 3 separated chambers connected by funnel-shaped microchannels. Cortical neurons are seeded in the proximal chamber, and axons reach the distal chamber after 4–6 d *in vitro*. An overpressured central channel enables optimal fluidic isolation and compartmentalized treatment between somatic and axonal compartments. *B)* Light microscope image of microchannels between proximal and distal chambers. *C–E)* Representative micrographs of somatic and axonal compartments after NMDA treatment. Cortical neurons were cultured for 11 d and treated for 24 h with 100 µM NMDA. Left: the somatodendritic compartment stained with anti-MAP2 (red) and Hoechst 33342 (blue). Asterisks denote condensed nuclei. Right: the axonal compartment stained with anti-β_3-tubulin: control condition $(\emptyset/\emptyset)$ *(C)*; somatodendritic treatment with NMDA (NMDA/$\emptyset$) *(D)*; and selective axonal treatment with NMDA ($\emptyset$/NMDA) *(E)*. Scale bars, 20 µm. *F)* Quantification of nuclear condensation in control and after compartmentalized NMDA treatment. Condensed nuclei were counted after Hoechst staining ($n = 3$). *G)* Quantification of AxD in control and after compartmentalized NMDA treatment ($n = 3$). Axonal fragmentation index was calculated as described in Methods. *H, I)* Effect of the NMDA antagonist MK-801 on NMDA-induced nuclear pyknosis and AxD: Cells were cotreated with 100 µM NMDA and 10/50 µM MK-801 in the somatodendritic compartment. Quantification of somatic status *(H)* and AxD *(I)* ($n = 3$). *$P < 0.05$.

with an elevated NAD^+ metabolome with NR as a neuroprotective compound, NR tended to elevate brain NAM and adenosine diphosphate receptor (ADPR), whereas no changes were evident in brains treated with NAD^+ (Fig. 2*H, I*).

NR has a local protective effect mainly restricted to the axonal compartment

Previous results have shown that NAD^+ delays Wallerian degeneration after axotomy on PNS-derived neuronal
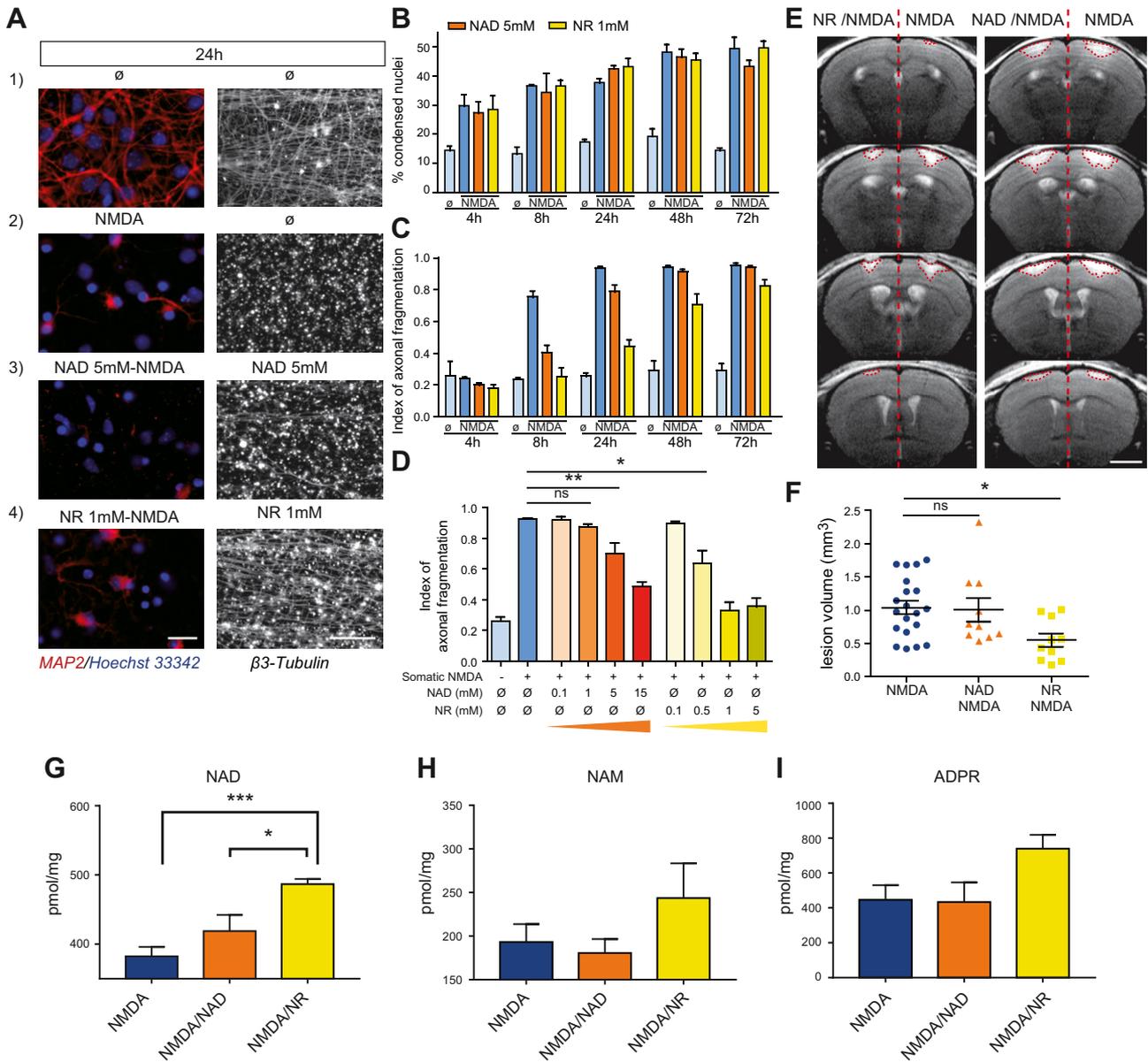
Figure 2. NR strongly prevents neurodegeneration induced by excitotoxicity both *in vitro* and *in vivo*. *A–D*) NAD^{+} weakly and NR strongly reduced NMDA-induced axonal degeneration. *A*) Fluorescence microscopic analysis of somatic status and AxD after a somatodendritic 100 μM NMDA treatment (24 h), with or without cotreatment with 5 mM NAD^{+} or 1 mM NR. Left: the somatodendritic compartment stained with Hoechst 33342 (blue) and anti-MAP2 (red) and the right picture shows the axonal compartment stained with anti-β3-tubulin: control condition (ø/ø) (*1*); somatodendritic treatment with NMDA (NMDA/ø) (*2*); somatodendritic cotreatment with NMDA and NAD^{+}, axonal treatment with NAD^{+} (NAD^{+}-NMDA/NAD^{+}) (*3*); and somatodendritic cotreatment with NMDA and NR, axonal treatment with NR (NR-NMDA/NR) (*4*). Scale bars, 20 μm. *B, C*) Effect of 5 mM NAD^{+} and 1 mM NR on neuronal death after different NMDA exposure times. *B*) Quantification of somatic status by condensed nuclei (%) after Hoechst staining (*n* = 3). *C*) Quantification of AxD (*n* = 3). *D*) Quantification of AxD on cortical neurons after 24 h of 100 μM NMDA and NR or NAD^{+} cotreatment. Dose responses of NR and NAD^{+} are shown (*n* = 3). *E, F*) *In vivo* neuroprotective effect of NR after intracranial NMDA administration in mice. *E*) Representative MRI images obtained 48 h after intracortical injection of 5 nmol NMDA or 5 nmol NMDA with 50 nmol NAD^{+} or NR. Lesion volume is outlined in red. Scale bar, 2 mm. *F*) Quantification of lesion volume at *t* = 48 h after NMDA injection (*n* = 20), NMDA/NAD^{+} injection (*n* = 10), and NMDA/NR injection (*n* = 10). *G–I*) Quantitative metabolomic analysis of NAD^{+} (*G*), NAM (*H*), and ADPR (*I*) of cortexes from mice injected with NMDA (*n* = 9), NMDA/NAD^{+} (*n* = 5), and NMDA/NR (*n* = 5). The data show that NR significantly elevated cortical NAD^{+}, whereas injected NAD^{+} did not. *P < 0.05, **P < 0.01, ***P < 0.001.

cells. Furthermore, both NAD^{+} and WldS protein prevent AxD in a soma-independent fashion (8, 41). Because NAD^{+} and NR protect AxD in our model, we examined if NAD^{+} and NR act locally at the axon or also depend on the somatic compartment. NAD^{+} or NR were applied either on both compartments or the somatodendritic or the axonal compartment simultaneously with somatodendritic addition of 100 μM NMDA for 24 h. Axonal application of NR partially protected axons from NMDA-induced degeneration (50% protection), whereas somatodendritic

application did not prevent it (**Fig. 3A–F**). Local NAD$^+$ treatment revealed no significant protective effects (Fig. 3G), but for both molecules NR and NAD$^+$, the protection was increased or detected when applied on both compartments together. These findings indicate that local axonal treatment with NR is required for axonal protection and that somatic NAD$^+$ or NR treatment is insufficient to fully prevent AxD. The data indicate that somatic application of these molecules helps to increase axonal protection induced by axonal application of the same compounds.

NR is converted to NAD$^+$ in cortical neurons

Not all models of WldS-dependent neuroprotection invoke a requirement for NAD$^+$ biosynthesis (42). Accordingly, we tested the hypothesis that the protective effect of NR depends upon its intracellular conversion to NAD$^+$ (**Fig. 4A**). First, we asked whether NR enters cortical neurons for further conversion to NAD$^+$. NR is a nucleoside reported to cross plasma membranes through NT (25, 27). Among NT isoforms, expression analysis in our neuronal cell culture model indicated that all equilibrative nucleoside transporter (ENT1-4) transcripts were expressed (Fig. 4B). However, none of the concentrative nucleoside transporter (CNT1-3) mRNAs could be detected. DP, a potent pharmacological inhibitor of ENT1 and -2 activities, blocks NR cell entry in human cell lines (25, 43). Cotreatment of cortical neurons with 100 µM NMDA, 1 mM NR, and 50 µM DP almost completely prevented NR-induced axonal protection (axonal protection decreased by 68%; from 88 to 20%), establishing that the neuroprotective effect of NR requires DP-sensitive transport through the plasma membrane (Fig. 4C).

Intracellular NR conversion to NAD$^+$ is initiated by Nmrk1/2, which generates the NAD$^+$-proximal precursor, NMN (Fig. 4A). We analyzed *Nmrk1* and -2 mRNA expression by quantitative RT-PCR from both specific mouse brain areas and from cortical neurons in culture. We discovered that *Nmrk1* mRNA is constitutively expressed in all tissues, whereas *Nmrk2* mRNA was absent in all brain areas (cortex, hippocampus, and cerebellum) (Fig. 4D, E). However, *Nmrk2* transcript was highly expressed in heart and striated skeletal muscles, as
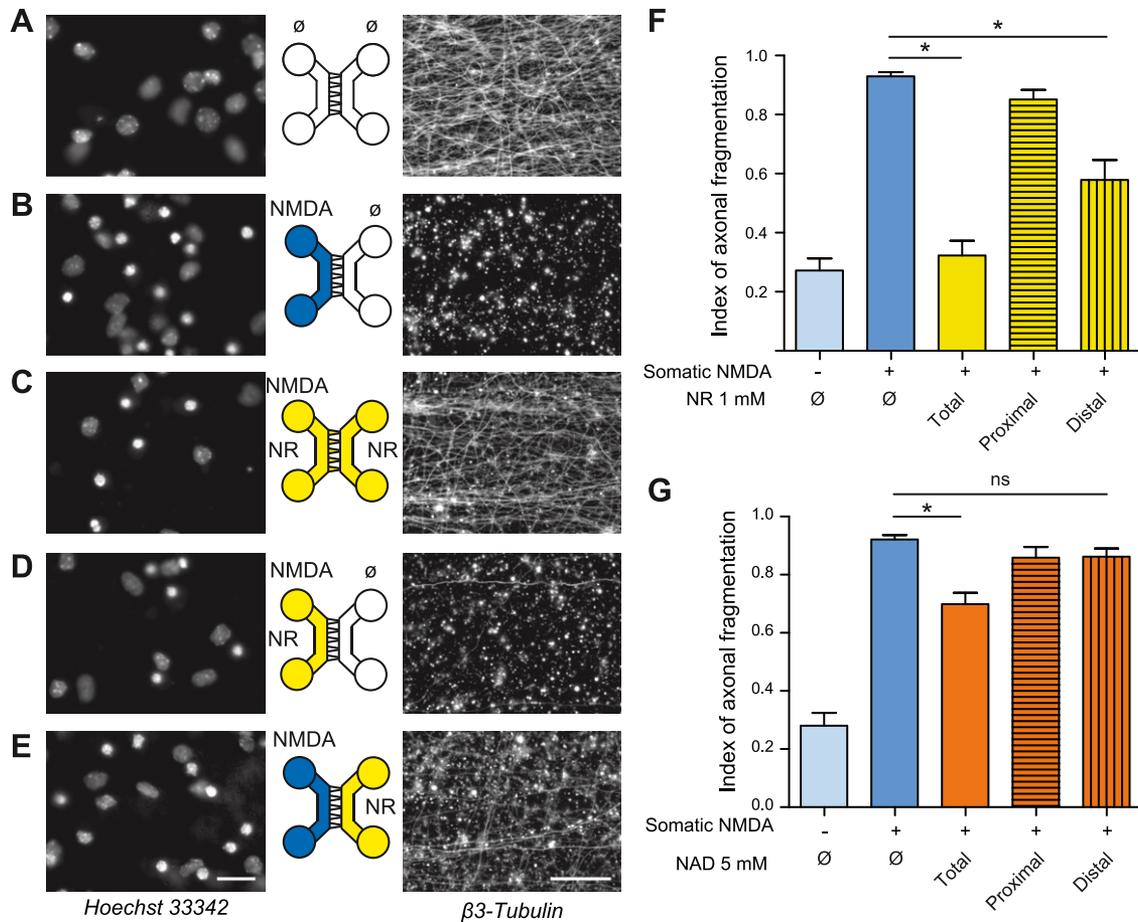

Figure 3. The NR protective effect is mainly restricted to the axonal compartment. *A–E*) Fluorescence microscopy analysis of somatic status and AxD after exposure of cortical neurons to 100 µM NMDA and 1 mM NR. Each molecule treatment was added for 24 h. Left: the somatic compartment stained with Hoechst 33342; right: the axonal compartment stained with anti-β3-tubulin. Control condition (ø/ø) (*A*); somatic NMDA treatment (NMDA/ø) (*B*); somatic NMDA-NR cotreatment and axonal NR treatment (NR-NMDA/NR) (*C*); somatic NR-NMDA cotreatment (NR-NMDA/ø) (*D*); and somatic NMDA treatment and axonal NR treatment (NMDA/NR) (*E*). Scale bars, 20 µm. *F, G*) Quantification of AxD after 100 µM NMDA treatment and total, proximal or distal 1 mM NR treatment (*F*) or 5 mM NAD$^+$ treatment (*G*) (*n* = 3). *$P < 0.05$.
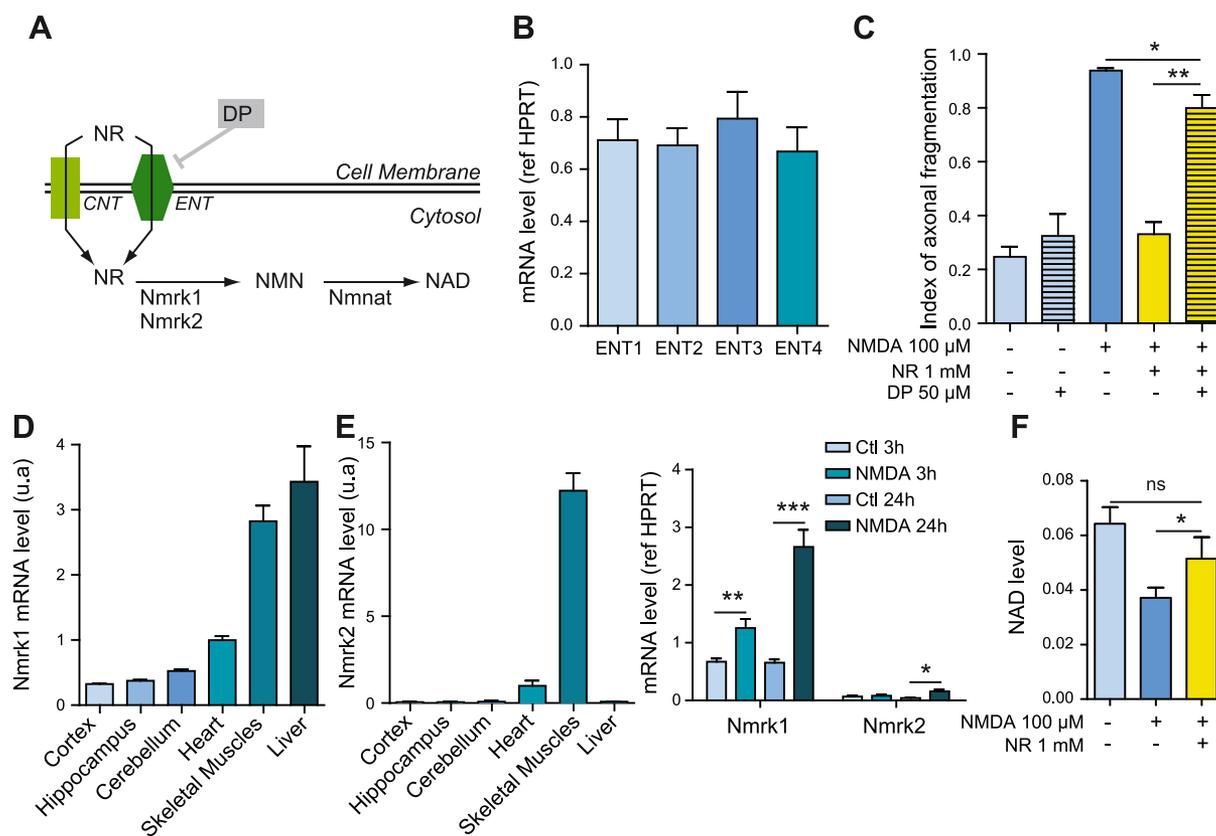
Figure 4. Extracellular NR is transported through the plasma membrane for a neuroprotective effect and is metabolized to intracellular NAD$^+$. *A*) Schematic representation of NR metabolism in cells: NR enters the cell through CNTs or ENTs and is metabolized to NAD$^+$ *via* NR kinase 1/2 (Nmrk1/2) and Nmnat. *B*) mRNA level of *ENT 1-4* normalized to *HPRT* transcript in cortical neurons. *C*) DP reverted the axon-protective effect of NR in neurons treated with NMDA. Quantification of AxD after 100 μM NMDA treatment, with or without 1 mM NR and 50 μM DP for 24 h (*n* = 4). *D*) *Nmrk1* mRNA is constitutively expressed, whereas *Nmrk2* mRNA is not detectable in brain tissues. *Nmrk1* and *Nmrk2* mRNA level in brain tissues (cortex, hippocampus, and cerebellum), heart, skeletal muscles, and liver normalized to β-actin transcript. *E*) NMDA treatment induces *Nmrk1* but not *Nmrk2* transcript. mRNA levels were analyzed by real-time quantitative PCR 3 and 24 h after 100 μM NMDA treatment and normalized to *HPRT* transcript (*n* = 3). *F*) NR treatment restores NMDA-induced NAD$^+$ depletion. The NAD$^+$ level was measured in cortical neurons cultured on plates and exposed to 100 μM NMDA, with or without 1 mM NR for 24 h (*n* = 4). *P < 0.05, **P < 0.01, ***P < 0.001.

previously described (30, 44). *Nmrk1* but not *Nmrk2* mRNA was also expressed in cultured cortical neurons (Fig. 4*E*). *Nmrk2* mRNA was reported to be induced in PNS neurons after sciatic nerve axotomy (7). To investigate a potential induction of Nmrk2 after an excitotoxic insult in cortical neurons, *Nmrk2* mRNA was quantified after 100 μM NMDA treatment for 24 h. We found a low induction of *Nmrk2* transcript, but a 4-fold increase of *Nmrk1* mRNA. NR kinase activity leads to formation of NMN, which is adenylylated to NAD$^+$ *via* Nmnat enzymes. We analyzed *Nmnat1-3* mRNA expression in cortical neurons treated or not with NMDA 100 μM for 3 or 24 h. We showed that all the transcripts are expressed, with the highest level for the cytosolic isoform Nmnat2, followed by the mitochondrial enzyme Nmnat3 (Supplemental Fig. S2*A*). Each of the mRNAs was induced by 24 h NMDA treatment such that all components of the NR kinase pathway to NAD$^+$ biosynthesis were upregulated during neuronal insult. NR conversion to NAD$^+$ can be initiated by nucleoside phosphorylase, which converts NR to NAM, which is further converted to NAD$^+$ (45). However, cotreatment

of cortical neurons with NMDA 100 μM and NAM 5 mM for 24 h demonstrated that NAM is unable to prevent NMDA-induced AxD (Supplemental Fig. S2*B*). We next evaluated NAD$^+$ levels in neurons during an excitotoxic challenge. Treatment of cortical neurons with 100 μM NMDA for 24 h induced a 36% decrease in intracellular NAD$^+$. This effect was reverted by cotreatment with 1 mM NR (Fig. 4*F*). Together, these results establish that conversion of NR to intracellular NAD$^+$ *via* the transcriptionally induced NR kinase pathway is critical for maintaining axoplasmic NAD$^+$ in opposition to excitotoxicity-induced AxD.

Extracellular NAD$^+$ involves a potentially unique mechanism to prevent excitotoxicity-induced AxD

Extracellular NAD$^+$ has a lower axon-protective effect than NR in our model. As reported previously in cell lines and PNS-derived neuronal cells, NAD$^+$ can be converted extracellularly to NMN by ENPPase and then to NR by 5′-ENTase (**Fig. 5***A*). We asked whether extracellular

conversion of NAD^+ to NR is necessary for NAD^+-mediated axonal protection or if this effect is independent of NR action. For this purpose, we probed 5'-ENTase activity in cortical neurons, using a high concentration of CMP, a competitive inhibitor of this enzyme (29). First, we treated cortical neurons with 100 μM NMDA, with or without 5 mM NMN for 24 h. Extracellular NMN significantly reduced NMDA-induced AxD and 25 mM CMP reversed the protective effect of NMN (Fig. 5B). Consistent with data in other tissues (28, 30), these data indicate that NMN must be converted to NR to mediate axonal protection. The beneficial effect of NMN was also prevented when cortical neurons were cotreated with NMDA and the ENT1/2 inhibitor DP, confirming that NMN is converted to the nucleoside NR before plasma membrane transport to prevent NMDA-induced AxD. Consistent with a dependence on conversion to NR, NR was more protective at a lower concentration than NMN. Surprisingly, 5 mM NAD^+ was slightly but significantly protective, yet neither CMP nor DP blocked the axonal protection conferred by this high concentration of NAD^+ (Fig. 5C).

NAD⁺ and NR protect neurons with the same efficiency after FK866-induced NAD⁺ depletion

Because excitotoxicity and SARM1 activation induce NAD^+ depletion in a manner that can be protected by NR and NAD^+, we tested whether pharmacological inhibition of NAD^+ homeostasis causes AxD. FK866, a specific inhibitor of Nampt (46), which salvages NAM for resynthesis of NAD^+ (**Fig. 6A**), was used to induce NAD^+ depletion. Addition of 10 μM FK866 to the somatodendritic compartment of cortical neurons induced a rapid decrease of NAD^+ levels after 24 h of treatment (Fig. 6B). At 72 h, this drop in NAD^+ induced somatodendritic degeneration, nuclear condensation, and AxD (Fig. 6C, D). Cotreatment of cortical neurons with 10 μM FK866 and 50 μM NAD^+ or NR fully prevented these effects (Fig. 6D–F). Notably,

the protective concentrations of NAD^+ and NR were lower than those used in the NMDA-induced neurodegeneration model (50 μM for both in the FK866 model and 5 mM NAD^+ or 1 mM NR in the NMDA model) (Figs. 2A–D and 6D–F). NAD^+ and NR remained fully protective when applied 24 h after treatment, at a time when NAD^+ depletion was already observed, but dropped to 20% protection when applied 48 h later (Fig. 6E, F). These findings highlight the existence of a temporal window in which neuronal integrity can be rescued after a neurotoxic insult. Taken together, these data show that NAD^+ and NR have the same neuroprotective effect against FK866-induced NAD^+ depletion.

Extracellular NAD⁺ conversion into NR is needed to prevent FK866-induced neurodegeneration

We next evaluated the metabolic pathway from extracellular NAD^+/NMN/NR to intracellular NAD^+ in FK866-induced neurodegeneration. First, cortical neurons were cotreated with 50 μM FK866, 50 μM NR, and 50 μM DP for 72 h, and axonal fragmentation was investigated. DP only partially limited the NR-protective effect against FK866 (axonal protection reduced by 40%), whereas the protective effect of NR was totally inhibited under NMDA stress (Figs. 4C and 7A). These data suggest that FK866 treatment induces expression of NT that is relatively resistant to DP. We analyzed *ENT1-4* mRNA in cortical neurons treated or not with 10 μM FK866 for 72 h. *ENT2* and *-4* mRNA were induced 2.2- and 1.7-fold, respectively, by FK866 (Supplemental Fig. S3). NAD^+ and NMN also prevented FK866-induced neurodegeneration in a manner that was partially prevented by DP (Fig. 7B, C). As NAD^+ may depend on NT in protection against FK866 neurodegeneration, we tested whether extracellular NAD^+ and NMN need to be converted to NR before transport through plasma membrane. Indeed, CMP fully blocked the axon-protective effect of NAD^+ and NMN, indicating
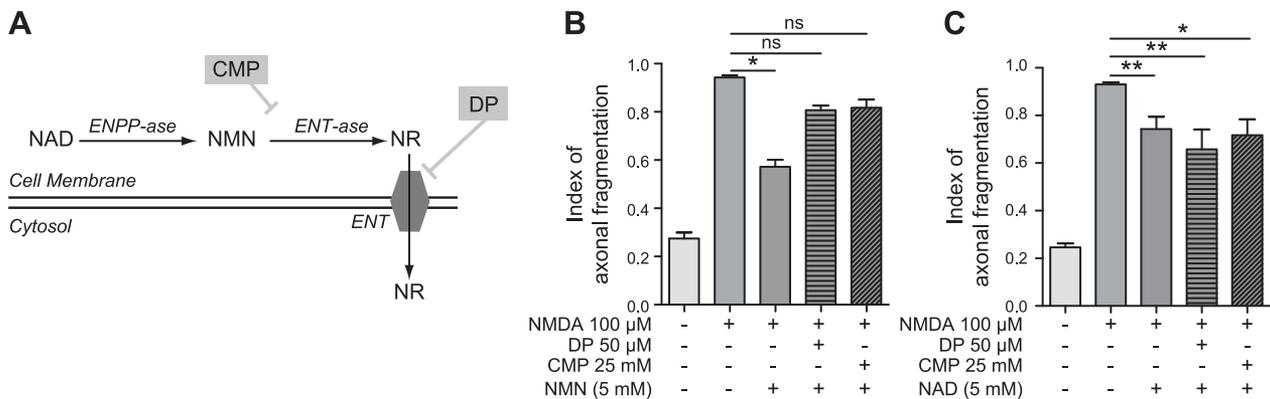

Figure 5. NMN requires conversion to NR and nucleoside transporters to prevent NMDA-induced AxD. *A*) Schematic representation of extracellular metabolism of NAD^+: NAD^+ is converted into NMN *via* ENPPase and then into NR *via* ENTase. *B*) Quantification of AxD in cortical neurons treated with 100 μM NMDA for 24 h after blocking the extracellular pathway by DP, an ENT inhibitor, or CMP, an ENTase inhibitor. NMDA, NMN, DP, and CMP were added as indicated (*n* = 3–7). *C*) Quantification of AxD in cortical neurons treated with 100 μM NMDA for 24 h after blocking the extracellular pathway by DP or CMP. NMDA, NAD^+, DP, and CMP were added as indicated (*n* = 3–7). *P < 0.05, **P < 0.01.
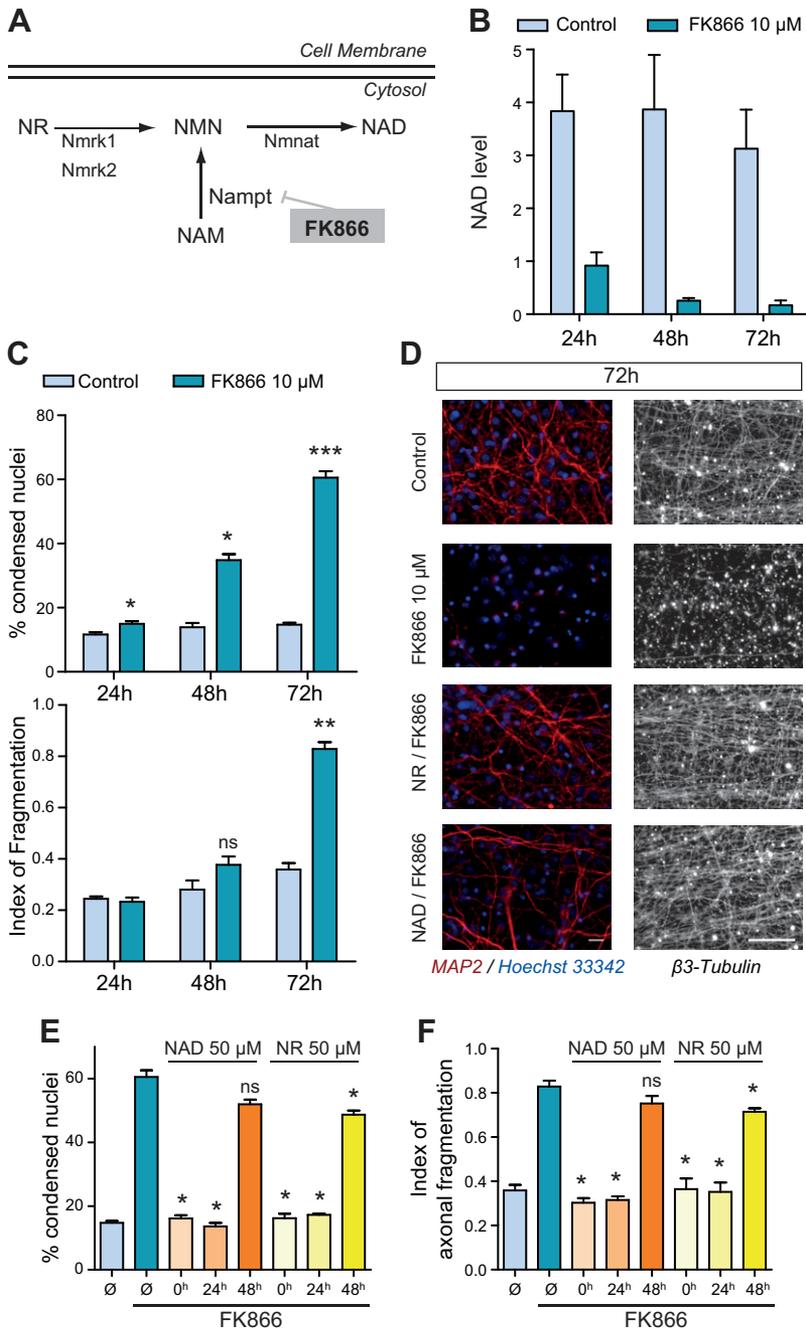
Figure 6. NAD^+ and NR have the same protective effect against FK866-induced cortical neurodegeneration. *A)* Schematic representation of FK866 effect on NAD^+ metabolism. *B)* NAD^+ level measured on cortical neurons cultured on plates exposed to 10 μM FK866 for 24, 48, and 72 h ($n = 3–4$). *C)* Quantification of somatic status and AxD in cortical neurons exposed to 10 μM FK866 ($n = 4$). *D)* Fluorescence microscopic analysis of somatic status and AxD after somatodendritic 10 μM FK866 treatment in the presence of 50 μM NAD^+ or 50 μM NR in both compartments (72 h). Left: the somatodendritic compartment stained with anti-MAP2 (red) and Hoechst 33342 (blue); right: the axonal compartment stained with anti-β3-tubulin. Scale bars, 20 μm. *E, F)* Effect of NR or NAD^+ on neuronal death and AxD in presence of FK866: cortical neurons where treated in both chambers with 50 μM NR or NAD^+ at the same time (0 h) or 24–48 h after 10 μM FK866 treatment for 72 h. *E)* Quantification of somatic status by percentage of condensed nuclei after Hoechst staining ($n = 3$). *F)* Quantification of AxD after β-tubulin staining ($n = 3$). *$P < 0.05$, **$P < 0.01$, ***$P < 0.001$.

that both molecules require 5′-ENTase activity to be converted to NR and mediate their axon-protective effect (Fig. 7*B, C*). We also analyzed *Nmrk1* and -*2* mRNA expression in cortical neurons treated or not with FK866 for 24–72 h. As expected, *Nmrk1* mRNA was highly expressed compared with the *Nmrk2* transcript, which was not detectable (Supplemental Fig. S4*B, C*). As previously described with NMDA, FK866 treatment for 48 or 72 h induced Nmrk2 (3-fold at 72 h). As Nmrk2 induction was a common phenomenon observed in our experiments, we used cortical neurons from wild-type or *Nmrk2*-KO mice. These neurons were treated with 10 μM FK866 for 72 h before condensed nuclei and axonal fragmentation were analyzed. Even in the absence of the *Nmrk2* gene, NAD^+ and NR provided full protection against FK866-induced neurodegeneration,

indicating that Nmrk2 is not required for these effects (Supplemental Fig. S4*D, E*). These results demonstrate that NAD^+, NMN, and NR use a similar pathway, likely independent of Nmrk2, to prevent FK866-induced neurodegeneration.

DISCUSSION

Excitotoxicity is a process commonly described in several brain disorders, including stroke, traumatic brain injuries, and the major neurodegenerative diseases. High glutamate release activates ionotropic glutamate receptor, as NMDAR, and triggers disruption of ion homeostasis, leading to energetic dysfunction and oxidative stress.
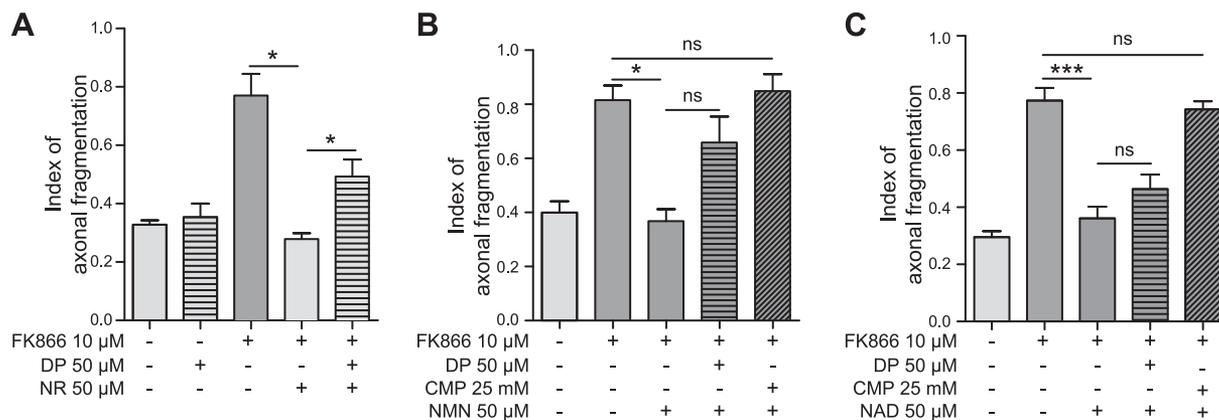
Figure 7. NAD$^+$ and NMN conversion to NR is needed to prevent FK866-induced AxD, and nucleoside transporters ENT-1/2 are partially involved. *A*) Quantification of AxD in cortical neurons treated with 10 μM FK866 for 72 h after blocking ENT1/2 by DP. FK866, NR, and DP were added as indicated ($n = 4$). *B*) Quantification of AxD in cortical neurons treated with 10 μM FK866 for 72 h after blocking the extracellular pathway by DP and CMP. FK866, NMN, DP, and CMP were added as indicated ($n = 3$). *C*) Quantification of AxD in cortical neurons treated with 10 μM FK866 for 72 h after blocking the extracellular pathway by DP and CMP. FK866, NAD$^+$, DP, and CMP were added as indicated ($n = 3–7$). *$P < 0.05$, ***$P < 0.001$.

Major events related to excitotoxicity are therefore mitochondrial dysfunction, NAD$^+$ depletion and metabolic dysregulation. Moreover, because neuronal stress induces DNA damages, poly (ADP-ribose) polymerase (PARP) activation, and NAD$^+$ depletion, the role of NAD$^+$ metabolism in excitotoxicity requires careful characterization (47).

Several *in vitro* studies examined the effect of NAD$^+$, its precursors, and biosynthetic enzymes in prevention of excitotoxicity-induced neuronal degeneration (17, 19, 23, 48–50). However, the results appeared to depend on particulars of the excitotoxicity models. For instance, exogenous NAM protects against neuronal degeneration after 6 or 12 h of glutamate/NMDA treatment, but not after 24 h (19). Furthermore, only weak neuroprotective effects of NAD$^+$ were observed after 100 μM glutamate application, even with NAD$^+$ doses up to 15 mM (23, 50). Our results showing that neither NAD$^+$ nor NR protects against NMDA-induced somatic degeneration are consistent with these studies. We discovered unexpectedly that NR and NAD$^+$ have differential effects on NMDA-induced AxD *in vitro* and *in vivo*. *In vitro*, 1 mM NR was highly efficient in preventing AxD, whereas 5 mM NAD$^+$ was partially protective. *In vivo*, injection of NR, but not NAD$^+$, significantly reduced NMDA-induced lesions (Fig. 2*E*, *F*) and elevated brain NAD$^+$ (Fig. 2*G*). We considered the possibility that NR coinjection altered the severity of the initial NMDA-triggered insult. One of the major initial neurotoxic events involved in NMDA receptor activation is a rise in intracellular calcium (51). Metabolomic analyses have shown that NR coinjection leads to ADPR induction (Fig. 2*H*, *I*). Actually, ADPR is known to enhance cytoplasmic calcium concentration, indicating that NR should enhance NMDA neurotoxicity, but this was not the case in this study, suggesting that NR injection reduces NMDA-induced lesion by acting downstream of the initial insult.

In PNS-derived neurons injured by axotomy, NR is protective reportedly because Nmrk2 is transcriptionally up-regulated by the injury (7). In the current study we showed that NR enters neurons *via* DP-sensitive transporters. Although Nmrk2 was slightly induced by NMDA or FK866 treatment (Fig. 4*E* and Supplemental Fig. S4*B*, *C*), Nmrk1 was more highly induced and NR prevented nuclear condensation and AxD in neurons from *Nmrk2*-KO mice treated with FK866 (Supplemental Fig. S4*D*, *E*). Thus, this result suggests that Nmrk1 is the key mediator of the neuroprotective activity of NR. Although NAD$^+$, NMN, or NR can break down to NAM, we found that NMDA-induced AxD is not prevented by NAM (Supplemental Fig. S2*B*).

In PNS-derived neurons injured by axotomy, the cytoplasmic NAD$^+$ biosynthetic enzyme Nmnat2 is reportedly unstable, leading to axonal NMN accumulation, which has been described as deleterious and accelerating AxD (27). However, NMN toxicity is not universally accepted, as it was reported that high levels of NMN are not sufficient to induce AxD in DRG neurons (16). In our model, no NMN or NR toxicity was observed. On the contrary, we report strong axonal protection with both molecules and an NR-identical intracellular mechanism for NMN consistent with inhibition by CMP and DP (Fig. 5). Moreover, we discovered that transcripts encoding Nmnat1–3 are all induced after 24 h of NMDA treatment (Supplemental Fig. S2*A*). Thus, the 2-step NR kinase pathway to NAD$^+$ (31) is induced by excitotoxic stress in cortical neurons. Nmnat2 protein subcellular localization and stability have been described to modulate the axon-protective capacity of this enzyme after axotomy in PNS-derived neurons (52), suggesting that enzyme regulation at the protein level is another important component of the response to NR.

Optimal NAD$^+$ and NR axon-protective effects were observed when the compounds were applied to both compartments, suggesting axonal protection can be assisted by a somatic signal. Mitochondria transport within the axon was recently shown to participate in axonal integrity (53). It will therefore be interesting to test whether NR promotes an increase in mitochondria biogenesis, the axonal transport of mitochondria, or both as a component of its neuroprotective effects.

Finally, we note that the effective concentrations of NR and NAD$^+$ for protection against two different models of cortical neurotoxicity were quite distinct. Whereas 1 mM or greater concentrations of NAD$^+$, NMN, and NR were necessary to protect against NMDA-induced AxD, 50 µM was sufficient to prevent FK866-induced neuronal degeneration (Figs. 2D, 6, and 7). We propose that the NMDA excitotoxic model induces SARM1 activation (13, 16, 54, 55) in a manner that leads to active NAD$^+$ depletion, whereas FK866 simply produces a block of the NAD$^+$ salvage pathway. The mechanisms involved in NAD$^+$ depletion are different, and some distinct pathways could be required to mediate both NAD$^+$ and NR protective effects. We have shown that NR-induced axonal protection was completely or partially prevented by DP in NMDA excitotoxicity and FK866 models, respectively (Figs. 4C and 7A). DP specifically inhibits ENT1/2 activities, but we have shown that all the transcripts coding the different ENT isoforms are expressed in cortical neurons (Fig. 4B). ENT3 is known to be an intracellular transporter predominantly localized in lysosome or mitochondria, whereas ENT4 is expressed at the plasma membrane and was described to be very abundant in brain and heart (56). FK866 treatment of cortical neurons induced ENT2 and -4 mRNA, suggesting that ENT4, which is not inhibited by DP, is involved in nucleoside transport when NAD$^+$ is highly depleted in neurons by FK866 (Supplemental Fig. S2A). Further mechanistic studies are under way to reveal the differences between FK866 and NMDA-induced cortical neurotoxicity. The human oral availability of NR (33) suggests the potential for testing NR in diseases and conditions of central neurodegeneration including Alzheimer's disease, Parkinson's disease, and traumatic brain injury. [FJ]

ACKNOWLEDGMENTS

AUTHOR CONTRIBUTIONS

P. Vaur, B. Brugg, and E. Duplus designed the research; P. Vaur performed all the experiments involving microfluidic chips and real-time quantitative PCR; M. Mericskay and Z. Li provided *Nmrk2*-KO mice and analyzed data; D. Vivien and C. Orset performed *in vivo* NMDA-induction experiments; B. Brugg and E. Jacotot analyzed data and participated in writing the manuscript; M. S. Schmidt and C. Brenner performed the metabolomic analysis; P. Vaur, C. Brenner, and E. Duplus analyzed data

and wrote the manuscript; and all authors read and approved the final manuscript.

REFERENCES

1. Benarroch, E. E. (2015) Acquired axonal degeneration and regeneration: recent insights and clinical correlations. *Neurology* **84**, 2076–2085

2. Burke, R. E., and O'Malley, K. (2013) Axon degeneration in Parkinson's disease. *Exp. Neurol.* **246**, 72–83

3. Kanaan, N. M., Pigino, G. F., Brady, S. T., Lazarov, O., Binder, L. I., and Morfini, G. A. (2013) Axonal degeneration in Alzheimer's disease: when signaling abnormalities meet the axonal transport system. *Exp. Neurol.* **246**, 44–53

4. Selkoe, D. J. (2002) Alzheimer's disease is a synaptic failure. *Science* **298**, 789–791

5. Araki, T., Sasaki, Y., and Milbrandt, J. (2004) Increased nuclear NAD biosynthesis and SIRT1 activation prevent axonal degeneration. *Science* **305**, 1010–1013

6. Magnifico, S., Saias, L., Deleglise, B., Duplus, E., Kilinc, D., Miquel, M. C., Viovy, J. L., Brugg, B., and Peyrin, J. M. (2013) NAD+ acts on mitochondrial SirT3 to prevent axonal caspase activation and axonal degeneration. *FASEB J.* **27**, 4712–4722

7. Sasaki, Y., Araki, T., and Milbrandt, J. (2006) Stimulation of nicotinamide adenine dinucleotide biosynthetic pathways delays axonal degeneration after axotomy. *J. Neurosci.* **26**, 8484–8491

8. Wang, J., Zhai, Q., Chen, Y., Lin, E., Gu, W., McBurney, M. W., and He, Z. (2005) A local mechanism mediates NAD-dependent protection of axon degeneration. *J. Cell Biol.* **170**, 349–355

9. Lyon, M. F., Ogunkolade, B. W., Brown, M. C., Atherton, D. J., and Perry, V. H. (1993) A gene affecting Wallerian nerve degeneration maps distally on mouse chromosome 4. *Proc. Natl. Acad. Sci. USA* **90**, 9717–9720

10. Coleman, M. P., and Freeman, M. R. (2010) Wallerian degeneration, wld(s), and nmnat. *Annu. Rev. Neurosci.* **33**, 245–267

11. Yahata, N., Yuasa, S., and Araki, T. (2009) Nicotinamide mononucleotide adenylyltransferase expression in mitochondrial matrix delays Wallerian degeneration. *J. Neurosci.* **29**, 6276–6284

12. Trammell, S. A., Weidemann, B. J., Chadda, A., Yorek, M. S., Holmes, A., Coppey, L. J., Obrosov, A., Kardon, R. H., Yorek, M. A., and Brenner, C. (2016) Nicotinamide riboside opposes type 2 diabetes and neuropathy in mice. *Sci. Rep.* **6**, 26933

13. Osterloh, J. M., Yang, J., Rooney, T. M., Fox, A. N., Adalbert, R., Powell, E. H., Sheehan, A. E., Avery, M. A., Hackett, R., Logan, M. A., MacDonald, J. M., Ziegenfuss, J. S., Milde, S., Hou, Y. J., Nathan, C., Ding, A., Brown, R. H., Jr., Conforti, L., Coleman, M., Tessier-Lavigne, M., Züchner, S., and Freeman, M. R. (2012) dSarm/Sarm1 is required for activation of an injury-induced axon death pathway. *Science* **337**, 481–484

14. Gerdts, J., Summers, D. W., Milbrandt, J., and DiAntonio, A. (2016) Axon self-destruction: new links among SARM1, MAPKs, and NAD+ metabolism. *Neuron* **89**, 449–460

15. Gilley, J., and Coleman, M. P. (2010) Endogenous Nmnat2 is an essential survival factor for maintenance of healthy axons. *PLoS Biol.* **8**, e1000300

16. Sasaki, Y., Nakagawa, T., Mao, X., DiAntonio, A., and Milbrandt, J. (2016) NMNAT1 inhibits axon degeneration via blockade of SARM1-mediated NAD(+) depletion. *eLife* **5**, e19749

17. Kim, S. H. Lu, H. F., and Alano, C. C. (2011) Neuronal Sirt3 protects against excitotoxic injury in mouse cortical neuron culture. *PLoS ONE* **6**, e14731

18. Liu, D., Pitta, M., and Mattson, M. P. (2008) Preventing NAD(+) depletion protects neurons against excitotoxicity: bioenergetic effects of mild mitochondrial uncoupling and caloric restriction. *Ann. N. Y. Acad. Sci.* **1147**, 275–282

19. Liu, D., Gharavi, R., Pitta, M., Gleichmann, M., and Mattson, M. P. (2009) Nicotinamide prevents NAD+ depletion and protects neurons against excitotoxicity and cerebral ischemia: NAD+ consumption by SIRT1 may endanger energetically compromised neurons. *Neuromolecular Med.* **11**, 28–42

20. Zhang, W., Xie, Y., Wang, T., Bi, J., Li, H., Zhang, L. Q., Ye, S. Q., and Ding, S. (2010) Neuronal protective role of PBEF in a mouse model of cerebral ischemia. *J. Cereb. Blood Flow Metab.* **30**, 1962–1971

21. Chung, R. S., McCormack, G. H., King, A. E., West, A. K., and Vickers, J. C. (2005) Glutamate induces rapid loss of axonal neurofilament proteins from cortical neurons in vitro. *Exp Neurol* **193**, 481–488

22. Hosie, K. A., King, A. E., Blizzard, C. A., Vickers, J. C., and Dickson, T. C. (2012) Chronic excitotoxin-induced axon degeneration in a compartment neuronal culture model. *ASN Neuro* **4**

23. Bi, J., Li, H., Ye, S. Q., and Ding, S. (2012) Pre-B-cell colony-enhancing factor exerts a neuronal protection through its enzymatic activity and the reduction of mitochondrial dysfunction in in vitro ischemic models. *J. Neurochem.* **120**, 334–346

24. Bogan, K. L., and Brenner, C. (2008) Nicotinic acid, nicotinamide, and nicotinamide riboside: a molecular evaluation of NAD+ precursor vitamins in human nutrition. *Annu. Rev. Nutr.* **28**, 115–130

25. Nikiforov, A., Dölle, C., Niere, M., and Ziegler, M. (2011) Pathways and subcellular compartmentation of NAD biosynthesis in human cells: from entry of extracellular precursors to mitochondrial NAD generation. *J. Biol. Chem.* **286**, 21767–21778

26. Grozio, A., Sociali, G., Sturla, L., Caffa, I., Soncini, D., Salis, A., Raffaelli, N., De Flora, A., Nencioni, A., and Bruzzone, S. (2013) CD73 protein as a source of extracellular precursors for sustained NAD+ biosynthesis in FK866-treated tumor cells. *J. Biol. Chem.* **288**, 25938–25949

27. Di Stefano, M., Nascimento-Ferreira, I., Orsomando, G., Mori, V., Gilley, J., Brown, R., Janeckova, L., Vargas, M. E., Worrell, L. A., Loreto, A., Tickle, J., Patrick, J., Webster, J. R. M., Marangoni, M., Carpi, F. M., Pucciarelli, S., Rossi, F., Meng, W., Sagasti, A., Ribchester, R. R., Magni, G., Coleman, M. P., and Conforti, L. (2015) A rise in NAD precursor nicotinamide mononucleotide (NMN) after injury promotes axon degeneration. *Cell Death Differ.* **22**, 731–742

28. Ratajczak, J., Joffraud, M., Trammell, S. A., Ras, R., Canela, N., Boutant, M., Kulkarni, S. S., Rodrigues, M., Redpath, P., Migaud, M. E., Auwerx, J., Yanes, O., Brenner, C., and Cantó, C. (2016) NRK1 controls nicotinamide mononucleotide and nicotinamide riboside metabolism in mammalian cells. *Nat. Commun.* **7**, 13103

29. Zimmermann, H. (2000) Extracellular metabolism of ATP and other nucleotides. *Naunyn Schmiedebergs Arch. Pharmacol.* **362**, 299–309

30. Fletcher, R. S., Ratajczak, J., Doig, C. L., Oakey, L. A., Callingham, R., Da Silva Xavier, G., Garten, A., Elhassan, Y. S., Redpath, P., Migaud, M. E., Philp, A., Brenner, C., Cantó, C., and Lavery, G. G. (2017) Nicotinamide riboside kinases display redundancy in mediating nicotinamide mononucleotide and nicotinamide riboside metabolism in skeletal muscle cells. *Mol. Metab.* **6**, 819–832

31. Bieganowski, P., and Brenner, C. (2004) Discoveries of nicotinamide riboside as a nutrient and conserved NRK genes establish a Preiss-Handler independent route to NAD+ in fungi and humans. *Cell* **117**, 495–502

32. Trammell, S. A., Yu, L., Redpath, P., Migaud, M. E., and Brenner, C. (2016) Nicotinamide riboside is a major NAD+ precursor vitamin in cow milk. *J. Nutr.* **146**, 957–963

33. Trammell, S. A., Schmidt, M. S., Weidemann, B. J., Redpath, P., Jaksch, F., Dellinger, R. W., Li, Z., Abel, E. D., Migaud, M. E., and Brenner, C. (2016) Nicotinamide riboside is uniquely and orally bioavailable in mice and humans. *Nat. Commun.* **7**, 12948

34. Gong, B., Pan, Y., Vempati, P., Zhao, W., Knable, L., Ho, L., Wang, J., Sastre, M., Ono, K., Sauve, A. A., and Pasinetti, G. M. (2013) Nicotinamide riboside restores cognition through an upregulation of proliferator-activated receptor-γ coactivator 1α regulated β-secretase 1 degradation and mitochondrial gene expression in Alzheimer's mouse models. *Neurobiol. Aging* **34**, 1581–1588

35. Brown, K. D., Maqsood, S., Huang, J. Y., Pan, Y., Harkcom, W., Li, W., Sauve, A., Verdin, E., and Jaffrey, S. R. (2014) Activation of SIRT3 by the NAD⁺ precursor nicotinamide riboside protects from noise-induced hearing loss. *Cell Metab.* **20**, 1059–1068

36. Hamity, M. V., White, S. R., Walder, R. Y., Schmidt, M. S., Brenner, C., and Hammond, D. L. (2017) Nicotinamide riboside, a form of vitamin B3 and NAD+ precursor, relieves the nociceptive and aversive dimensions of paclitaxel-induced peripheral neuropathy in female rats. *Pain* **158**, 962–972

37. Deleglise, B., Lassus, B., Soubeyre, V., Alleaume-Butaux, A., Hjorth, J. J., Vignes, M., Schneider, B., Brugg, B., Viovy, J. L., and Peyrin, J. M. (2013) Synapto-protective drugs evaluation in reconstructed neuronal network. *PLoS One* **8**, e71103

38. Trammell, S. A., and Brenner, C. (2013) Targeted, LCMS-based metabolomics for quantitative measurement of NAD(+) metabolites. *Comput. Struct. Biotechnol. J.* **4**, e201301012

39. Paxinos G., and Franklin K. (2012) *Paxinos and Franklin's the Mouse Brain in Stereotaxic Coordinates.* 4th ed. Academic Press, Cambridge, MA, USA

40. Jullienne, A., Montagne, A., Orset, C., Lesept, F., Jane, D. E., Monaghan, D. T., Maubert, E., Vivien, D., and Ali, C. (2011) Selective inhibition of GluN2D-containing N-methyl-D-aspartate receptors prevents tissue plasminogen activator-promoted neurotoxicity both in vitro and in vivo. *Mol. Neurodegener.* **6**, 68

41. Cohen, M. S., Ghosh, A. K., Kim, H. J., Jeon, N. L., and Jaffrey, S. R. (2012) Chemical genetic-mediated spatial regulation of protein expression in neurons reveals an axonal function for wld(s). *Chem. Biol.* **19**, 179–187

42. Antenor-Dorsey, J. A. V., and O'Malley, K. L. (2012) WldS but not Nmnat1 protects dopaminergic neurites from MPP+ neurotoxicity. *Mol. Neurodegener.* **7**, 5

43. Griffith, D. A., and Jarvis, S. M. (1996) Nucleoside and nucleobase transport systems of mammalian cells. *Biochim. Biophys. Acta* **1286**, 153–181

44. Cantó, C., Houtkooper, R. H., Pirinen, E., Youn, D. Y., Oosterveer, M. H., Cen, Y., Fernandez-Marcos, P. J., Yamamoto, H., Andreux, P. A., Cettour-Rose, P., Gademann, K., Rinsch, C., Schoonjans, K., Sauve, A. A., and Auwerx, J. (2012) The NAD(+) precursor nicotinamide riboside enhances oxidative metabolism and protects against high-fat diet-induced obesity. *Cell Metab.* **15**, 838–847

45. Belenky, P., Racette, F. G., Bogan, K. L., McClure, J. M., Smith, J. S., and Brenner, C. (2007) Nicotinamide riboside promotes Sir2 silencing and extends lifespan via Nrk and Urh1/Pnp1/Meu1 pathways to NAD+. *Cell* **129**, 473–484

46. Hasmann, M., and Schemainda, I. (2003) FK866, a highly specific noncompetitive inhibitor of nicotinamide phosphoribosyltransferase, represents a novel mechanism for induction of tumor cell apoptosis. *Cancer Res.* **63**, 7436–7442

47. Martire, S., Mosca, L., and d'Erme, M. (2015) PARP-1 involvement in neurodegeneration: a focus on Alzheimer's and Parkinson's diseases. *Mech. Ageing Dev.* **146–148**, 53–64

48. Ghosh, D., LeVault, K. R., Barnett, A. J., and Brewer, G. J. (2012) A reversible early oxidized redox state that precedes macromolecular ROS damage in aging nontransgenic and 3xTg-AD mouse neurons. *J. Neurosci.* **32**, 5821–5832

49. Verghese, P. B., Sasaki, Y., Yang, D., Stewart, F., Sabar, F., Finn, M. B., Wroge, C. M., Mennerick, S., Neil, J. J., Milbrandt, J., and Holtzman, D. M. (2011) Nicotinamide mononucleotide adenylyl transferase 1 protects against acute neurodegeneration in developing CNS by inhibiting excitotoxic-necrotic cell death. *Proc. Natl. Acad. Sci. USA* **108**, 19054–19059

50. Wang, X., Li, H., and Ding, S. (2014) The effects of NAD+ on apoptotic neuronal death and mitochondrial biogenesis and function after glutamate excitotoxicity. *Int. J. Mol. Sci.* **15**, 20449–20468

51. Choi, D. W. (1987) Ionic dependence of glutamate neurotoxicity. *J. Neurosci.* **7**, 369–379

52. Milde, S., Gilley, J., and Coleman, M. P. (2013) Subcellular localization determines the stability and axon protective capacity of axon survival factor Nmnat2. *PLoS Biol.* **11**, e1001539

53. Zhou, B., Yu, P., Lin, M. Y., Sun, T., Chen, Y., and Sheng, Z. H. (2016) Facilitation of axon regeneration by enhancing mitochondrial transport and rescuing energy deficits. *J. Cell Biol.* **214**, 103–119

54. Gerdts, J., Summers, D. W., Sasaki, Y., DiAntonio, A., and Milbrandt, J. (2013) Sarm1-mediated axon degeneration requires both SAM and TIR interactions. *J. Neurosci.* **33**, 13569–13580

55. Gerdts, J., Brace, E. J., Sasaki, Y., DiAntonio, A., and Milbrandt, J. (2015) SARM1 activation triggers axon degeneration locally via NAD⁺ destruction. *Science* **348**, 453–457

56. Young, J. D. (2016) The SLC28 (CNT) and SLC29 (ENT) nucleoside transporter families: a 30-year collaborative odyssey. *Biochem. Soc. Trans.* **44**, 869–876